A MOMENT METHOD FORMULATION FOR THE ANALYSIS OF WIRE ANTENNAS ATTACHED TO ARBITRARY CONDUCTING BODIES DEFINED BY PARAMETRIC SURFACES

F. Rivas, L. Valle and M.F. Cátedra
Departamento de Ingeniería de Comunicaciones, Universidad de Cantabria,
Avda. Los Castros s/n. 39005 Santander, Cantabria, SPAIN

ABSTRACT. A Moment Method (MM) technique for the analysis of wire antennas on board resonant-sized bodies modelled with parametric surfaces is presented. The approach may have useful applications for the study of the behaviour of wire antennas on board complex conducting structures like aircrafts. The current is represented by curved rooftop functions on the body, piecewise linear functions on the wires and a new junction function in the attachment region between the body and the antenna. The bodies are precisely defined by means of a small number of NURBS surfaces (Non Uniform Rational B-Splines) and Bézier patches (BP). In addition the new junction function that can be defined over any BP allows the antenna to be attached to any part of the body. Radiation patterns and input impedance calculations for several geometries are presented to show the accuracy of the method. The results are successfully validated when comparisons with measurements or results from other methods are carried out.

1 INTRODUCTION

The MM [1] is one of the most popular techniques for the analysis of electromagnetic scattering of arbitrary bodies of small or resonant size. The method gives good results when analyzing wire antennas and can be used to obtain the scattering field by surfaces represented by wire grid models [2]. However, the wire grid modelling does not work properly when near-field parameters such as input impedances or current distributions are calculated. Subsequently, a surface representation of the conducting bodies must be introduced.

A representation of the bodies by flat triangular or rectangular patches provides excellent results of near and far-field parameters for many problems, however it presents the disadvantage that high amounts of memory and CPU-times are needed when the geometry is electrically large. These problems can be substantially reduced by defining the MM basis functions directly over the models of the bodies based on meshes of NURBS surfaces and BP [3] because fewer number of patches are needed to represent the body accurately.

NURBS surfaces are B-Spline elements formed by a set of patches defined by polynomials, [3]. The coefficients of these polynomials depend on merely a few control points (see Fig.1). A body that is quite complex, for instance a complete aircraft, can be modelled with nearly all its details by only a few hundred NURBS. Any NURBS can be expressed in terms of BP. NURBS surfaces are more efficient for representing and storing the information necessary for describing a geometry however BP are more suitable for the numerical computation of parameters associated with the local behaviour of a surface like curvatures, derivatives, etc. It is a fast and easy process to obtain the BP from a NURBS representation by applying the Cox-de Boor transformation algorithm [4].

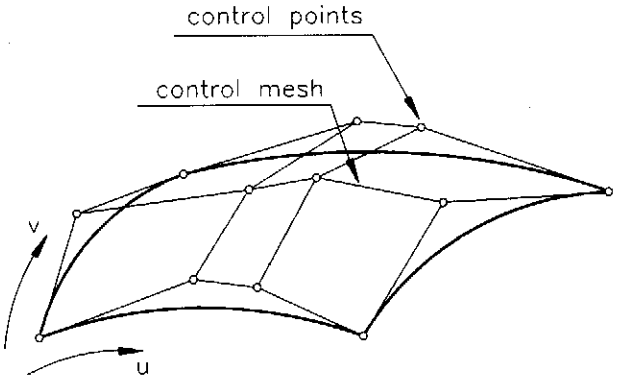

Figure 1. NURBS surface and its associated control points

In a previous paper [5] the authors presented a MM technique using NURBS surfaces and BP to represent the geometry of arbitrarily shaped scatterers. Modelling using that method implies that fewer basis functions are needed to obtain a precise representation of complex bodies. In that approach a new basis function associated with each boundary line between pairs of adjacent BP was introduced. These basis functions can be considered a generalization of the planar rooftop functions introduced by Glisson [6]. Curved "razor-blade" functions were considered as testing functions. This method was successfully validated when RCS values of several objects were obtained and compared with available data from other methods.

The purpose of this paper is to present an extension of the method mentioned above in order to analyze antennas

mounted over conducting surfaces. By establishing continuity of current at the wire-surface junction, a new special basis function (attachment or junction subdomain) has been introduced. This junction subdomain extends over a BP of the model and a segment of the attached wire antenna. This new subdomain presents an added advantage compared with previous works that can be attached to any of the BP of the body model. As the BP can be of complex shape it is possible to connect the antenna to any part of the body. Moreover the wire attachment itself need not be taken into account when the body is modelled. Therefore our formulation derived from the use of NURBS and BP allows us to consider more complex bodies and attachment points than in previously published works, [7-9].

This paper is organized as follows: Part 2 presents the description of the proposed MM scheme, giving an overview of the basis and testing functions used, the junction subdomain, the electrical fed model and the computation of the MM matrix terms; Part 3 presents the radiation patterns and input impedances for several canonical objects including comparisons with results obtained by other methods or measurements; the conclusions are outlined in Part IV.

2 FORMULATION

The electric current is represented by three kinds of basis functions depending on the part of the geometry considered: generalized curved rooftops over the BP that describe the body surface, piecewise triangular functions on the wire antennas and junction subdomains in the wire-surface attachment area.

2.1 Generalized curved rooftops

The body is modelled by means of meshes of NURBS surfaces that are subdivided into BP. A basis function is assigned to each one of the boundary lines between pairs of adjacent BP; each basis function extends only over the pair of patches that share a common boundary line. A constant charge density is imposed on the BP, [5]. Curved razor-blade functions, defined over the isoparametric lines which join the centres of the pair of BP associated with each basis function have been considered as testing functions.

2.2 Wire antennas

A thin wire approximation has been used, assuming that the radius of the antennas is much smaller than the length. Although the wires can be arbitrarily curved, a piecewise linear approximation is made by connecting straight cylindrical sections as can be seen in Fig.2. Triangle and pulse functions have been chosen as basis and testing functions, respectively. A procedure which bears a considerable resemblance to that proposed in [6] has been considered for the numerical treatment of the MM terms.

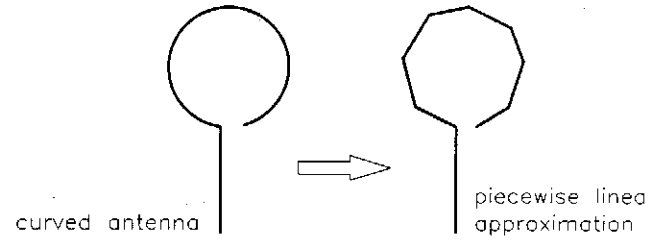

Figure 2. Curved antennas subdivided into a set of cylindrical straight segments

2.3 Attachment subdomain

This new subdomain extends over a wire segment and over a BP, as can be seen in Fig.3. The wire segment is assumed electrically short (e.g. $\lambda/36$ long) and normal to the surface (the other wire segments can be arbitrarily oriented). The current associated with the junction subdomain is a piecewise linear function (semi-triangle) on the wire and it is assumed that the current flows approximately radially from the attachment point on the BP. A total charge of $-1/j\omega$ on the wire (where ω is the radian frequency) and a charge of $1/j\omega$ on the patch are imposed. The charge continuity equation ($I = -j\omega q$) tells us that the total current of the junction subdomain is 1 Ampere. The charge density is assumed to be constant in both wire segment and surface patch. The exact shape of the current density on the BP of the junction subdomain is neither defined nor computed. The only imposition is that the charge density should be a constant function with a total charge of $1/j\omega$. As we will see below it is not necessary to know the exact shape of the current on the BP of the junction subdomain.

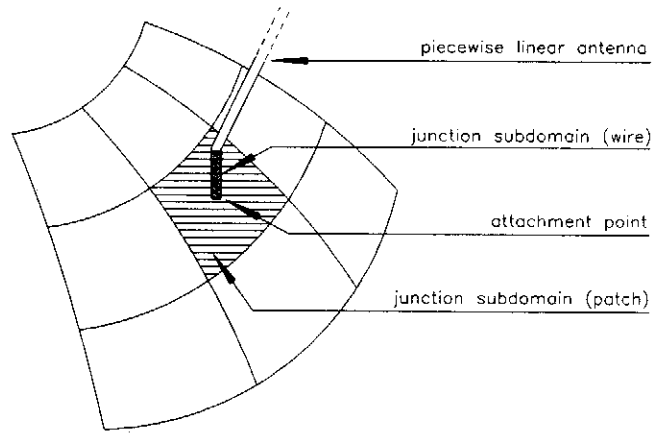

Figure 3. The junction subdomain formed by a wire segment and a Bézier patch

Fig.4 shows the shape of the testing function for the junction subdomain. A pulse function is defined as a testing function solely on the wire part of the junction subdomain. No testing is made in the patch surface of the junction subdomain because this patch is a part of the body geometry. It has been tested by the weighting functions associated with the generalized rooftop functions employed for the body, [5].

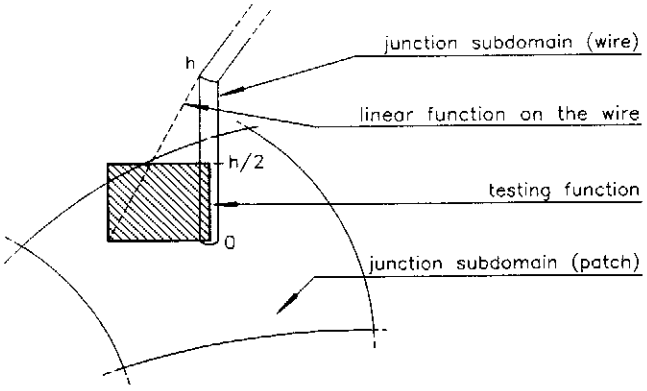

Figure 4. Testing functions for the junction subdomain

It is important to note that since one part of the junction subdomain is one patch of the NURBS meshing (not an additional disc or a flat patch), the connection of an antenna to the body does not imply any restriction or modification in the NURBS meshing. The sole restriction for the attachment points is that they should be positioned in or near the centre of a BP. This is not an important limitation because the junction patches are or can be made electrically small (typically a body is modelled using four to six patches per wavelength in its curved areas or eight to ten in its flat parts). In fact, this restriction is inherent to the discretization process of the problem that appears when using a numerical method like MM. In other words we must accept a quantization effect for the possible position where the wire can be placed. When attaching a wire antenna to a patch model of a body, two points on its surface are considered different only if they do not belong to the same BP.

2.4 MM coupling matrix

The objective is to solve the electric field integral equation (EFIE). To do that, the current density $\vec{J}$ is expressed as a sum of the current density on each subdomain as:

$$\vec{J}(\vec{r}) = \sum_{i=1}^{B} \vec{J}_i^{\,b}(\vec{r}) + \sum_{i=1}^{W} \vec{J}_i^{\,w}(\vec{r}) + \sum_{i=1}^{U} \vec{J}_i^{\,u}(\vec{r}) \qquad (1)$$

where B is the number of subdomains over the patches of the geometry modelled with NURBS surfaces, W is the number of subdomains defined on all the wire antennas of the problem and U is the number of junction subdomains. Then, the EFIE for this problem takes the form:

$$\hat{n}\times\vec{E}^{\,inc}(\vec{r}) = \hat{n}\times\sum_{i=1}^{B} \mathcal{L}\left[\vec{J}_i^{\,b}(\vec{r})\right] + \hat{n}\times\sum_{i=1}^{W} \mathcal{L}\left[\vec{J}_i^{\,w}(\vec{r})\right] + \hat{n}\times\sum_{i=1}^{U} \mathcal{L}\left[\vec{J}_i^{\,u}(\vec{r})\right] \qquad (2)$$

where $\vec{E}^{\,inc}(\vec{r})$ represents the impressed electric field, $\hat{n}$ is the normal vector and the integro-differential operator $\mathcal{L}\left[\vec{J}_i(\vec{r})\right]$ is defined by:

$$\mathcal{L}\left[\vec{J}_i(\vec{r})\right] = \frac{j\omega\mu}{4\pi}\int_S \vec{J}_i(\vec{r}\,')\,G(\vec{r},\vec{r}\,')\,dS' - \frac{1}{j\omega 4\pi\varepsilon}\nabla\int_S \nabla_s\vec{J}_i(\vec{r}\,')\,G(\vec{r},\vec{r}\,')\,dS' \qquad (3)$$

Equation (2) is converted into an equivalent set of linear equations. The coefficients of this system form the MM impedance matrix that can be grouped in nine boxes:

$$\begin{pmatrix} Z^{uu} & Z^{uw} & Z^{ub} \\ Z^{wu} & Z^{ww} & Z^{wb} \\ Z^{bu} & Z^{bw} & Z^{bb} \end{pmatrix}$$

where u denotes a junction subdomain, w a subdomain on a wire and b a subdomain on the body.

Since the objective of this paper is to introduce the connection between wires and surfaces, only the terms related with junction subdomains will be addressed in detail. The matrix terms related to the wire antennas have been treated by other authors, for instance [7-9] and those related to the subdomains over BP were introduced in [5].

If we consider the coupling between the i and the j-junction subdomains, we are referring to one of the terms of the Z^{uu} box of the MM matrix. This term is obtained by evaluating the expression:

$$Z^{uu}(i,j) = \left\langle T_i^{\,u}, \mathcal{L}\left[J_j^{\,u}\right]\right\rangle \qquad (4)$$

where T_i^u is the testing function associated with the i-junction subdomain (see Fig.4). This last expression can be computed as a sum of one inductive and one capacitive term depending on the potential vector and potential scalar of the j-subdomain, respectively.

The inductive term of (4) is given by the expression:

$$Z_{ind}^{uu}(i,j) = \frac{j\omega\mu}{4\pi} \int_0^{h_i^u/2} \left[\int_{S_{w_j}^u} J_w(\vec{r}\,') G(\vec{r},\vec{r}\,') dS' + \int_{S_{S_j}^u} J_s(\vec{r}\,') G(\vec{r},\vec{r}\,') dS' \right] d\vec{l} \quad (5)$$

where the current densities on the junction subdomain j have been separated into two parts depending on which part of this subdomain we are considering: $J_w(\vec{r}\,')$ on the surface of the wire segment ($S_{w_j}^u$) and $J_S(\vec{r}\,')$ on the surface of the BP ($S_{S_j}^u$). The inductive term defined in (5) can be largely simplified: a) if we neglect the contribution of the BP current because as J_S is approximately radial its equivalent momentum vanishes; b) if we approximate the current J_w by a pulse function that extends over the first half of the segment of the junction subdomain j and c) if we consider the inductive field to be constant along the wire segment over which the testing function of the i subdomain extends. The simplified expression as follows:

$$Z_{ind}^{uu}(i,j) \approx \frac{j\omega\mu}{4\pi} \frac{h_i^u}{2} \hat{dl}_i \cdot \int_0^{h_j^u/2} G(\vec{r}_{hi},\vec{r}\,') d\vec{l}' \quad (6)$$

where $\vec{r}_{hi}$ is the centre point of the wire segment corresponding to the i-junction subdomain. On the other hand, the capacitive term of (4) can be obtained as:

$$Z_{cap}^{uu}(i,j) = \frac{1}{4\pi\varepsilon} \int_0^{h_i^u/2} \nabla \left[\int_{S_{w_j}^u} \rho(\vec{r}\,') G(\vec{r},\vec{r}\,') dS' + \int_{S_{S_j}^u} \sigma(\vec{r}\,') G(\vec{r},\vec{r}\,') dS' \right] d\vec{l} \quad (7)$$

where $\rho(\vec{r}\,')$ and $\sigma(\vec{r}\,')$ are the charge densities on the wire segment and on the BP surface of the junction subdomain j, respectively. Taking into account the fact that these densities are constant and that the total charge in the surfaces is equal to $1/j\omega$ we have:

$$Z_{cap}^{uu}(i,j) = \frac{-1}{4\pi\varepsilon j\omega} \int_0^{h_i^u/2} \nabla \left[\frac{1}{h_j^u} \int_0^{h_j^u} G(\vec{r},\vec{r}\,') dl' - \frac{1}{S_{S_j}^u} \int_{S_{S_j}^u} G(\vec{r},\vec{r}\,') dS' \right] d\vec{l} \quad (8)$$

Taking into account that:

$$\int_a^b \nabla f(r)\, dr = f(b) - f(a) \quad (9)$$

expression (8) can be re-written as:

$$Z_{cap}^{uu}(i,j) = \frac{-1}{4\pi\varepsilon j\omega} \left[f\left(h_i^u/2\right) - f(0) \right] \quad (10)$$

where the function f is defined as:

$$f(l) = \frac{1}{h_j^u} \int_0^{h_j^u} G(\vec{r},\vec{r}\,') dl' \Big|_{r=l} - \frac{1}{S_{S_j}^u} \int_{S_{S_j}^u} G(\vec{r},\vec{r}\,') dS' \Big|_{r=l} \quad (11)$$

Similar expressions for the rest of terms of the MM matrix can be obtained considering the domain and the limits of integration in each case. Thus, the capacitive and inductive term of the coefficient $Z^{uw}(i,j)$ are expressed as:

$$Z_{ind}^{uw}(i,j) = \frac{j\omega\mu}{4\pi} \int_0^{h_i/2} \left[\int_{l_j} J_a(\vec{r}\,') G(\vec{r},\vec{r}\,') dl' \right] d\vec{l} \quad (12a)$$

$$Z_{cap}^{uw}(i,j) = \frac{-1}{4\pi\varepsilon j\omega} \int_0^{h_i/2} \nabla \left[\int_{l_j} \nabla' J_a(\vec{r}\,') G(\vec{r},\vec{r}\,') dl' \right] d\vec{l} \quad (12b)$$

where l_j is the wire segment of the j-antenna subdomain and J_a represents the current on that subdomain.

If it is assumed that the j subdomain of the body is shared by the Bézier's patches A and B, being J_b^A and J_b^B the current of the basis function on both patches respectively, the coefficient $Z^{ub}(i,j)$ is defined as:

$$Z_{ind}^{ub}(i,j) = \frac{j\omega\mu}{4\pi}\int_0^{h_i/2}\left[\int_{S_A} J_b^A(\vec{r}')\,G(\vec{r},\vec{r}')\,dS' + \int_{S_B} J_b^B(\vec{r}')\,G(\vec{r},\vec{r}')\,dS'\right]d\vec{l} \quad (13a)$$

$$Z_{cap}^{ub}(i,j) = \frac{-1}{4\pi\epsilon j\omega}\int_0^{h_i/2}\nabla\left[\int_{S_B} G(\vec{r},\vec{r}')\,dS' - \int_{S_A} G(\vec{r},\vec{r}')\,dS'\right]d\vec{l} \quad (13b)$$

where S_A and S_B are the areas of the patches A and B.

Finally, all the integral involved in the expressions for the coupling impedances are carried out numerically by means of the Gauss' Quadrature Method. This algorithm avoids the singularity of the Green's function which occurs when the points $\vec{r}$ and $\vec{r}'$ coincides. Because of this, the expressions developed above hold for the self-terms.

In the study presented in this paper the magnetic current frill model is used to feed the antennas. For this purpose, a voltage of *1* volt is distributed among the subdomains which share the BP where the wire is attached, as shown in Fig.5. This figure shows the digitized impressed voltage which is associated to each one of these subdomains to approximately model the magnetic current frill.

3 RESULTS

Several geometries have been analyzed in order to validate the method presented. The results include examples of monopole antennas attached to perfectly conducting bodies such as spheres, cylinders and other ground planes. Radiation patterns and input impedance values have been obtained and compared with measurements or results from other methods.

3.1 Monopole on conducting sphere

Figs.6-7 shows a quarterwave monopole antenna on a conducting sphere. Computed results for $a=\lambda/4$ and $a=\lambda/8$, are presented (solid line) and compared with those taken from [10]. The sphere has been modelled by a mesh of BP that form *4* meridians and *9* parallel lines (*76* basis functions on the sphere). Good agreement is observed in both cases. It is important to notice that, since the sphere is a body of revolution, the patches on the poles are triangular and considerably smaller than the remaining patches but no special treatment of the current has been applied.

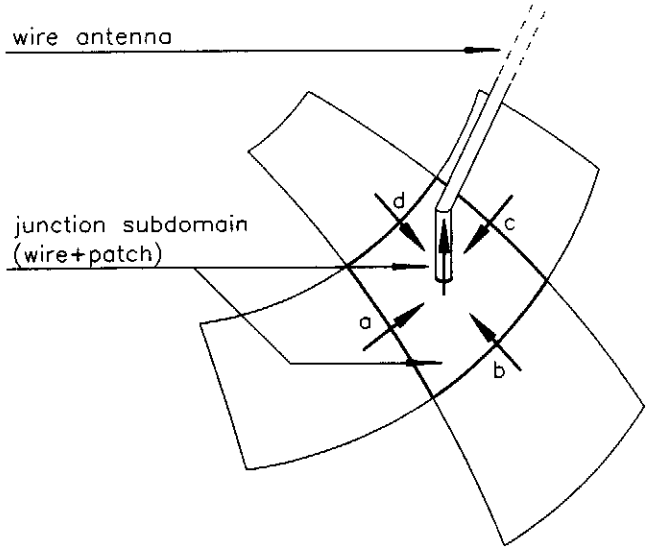

Figure 5. Feeding model for the attached antenna. An impressed voltage of *0.5* Volts is imposed on the junction subdomain and on the regular surface subdomain *a, b, c* and *d* that surrounds the antenna

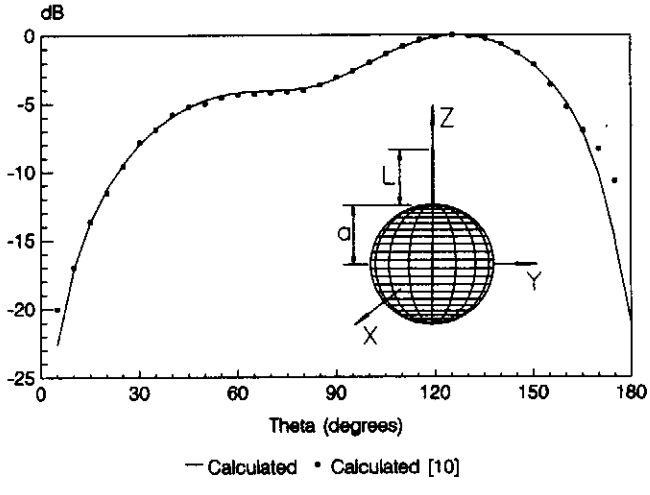

Figure 6. Radiation pattern of an $\lambda/4$ monopole on a $\lambda/4$ sphere

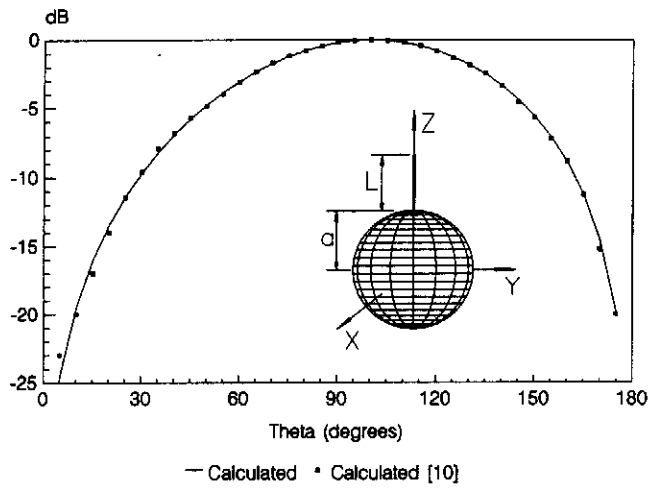

Figure 7. Radiation pattern of an $\lambda/4$ monopole on a $\lambda/8$ sphere

3.2 Monopole on a conducting cylinder

Fig.8 shows the configuration of a monopole antenna (A) diametrically opposite a passive boom (B) on the surface of a cylinder of height and diameter *0.22m* and *0.20m* respectively. The wavelength is *0.36m*. Computed values (solid line) for the $\phi=0^o$ cut are compared in Fig.8 with measured data (points) taken from [8] for a monopole length = *0.08m* and a boom length = *0.44m*. Assuming that the z-axis coincides with the cylinder axis, the mesh of BP of the cylinder is defined by *12* equidistant meridian lines (ϕ-constant curves) and *5* parallel lines (z-constant curves).

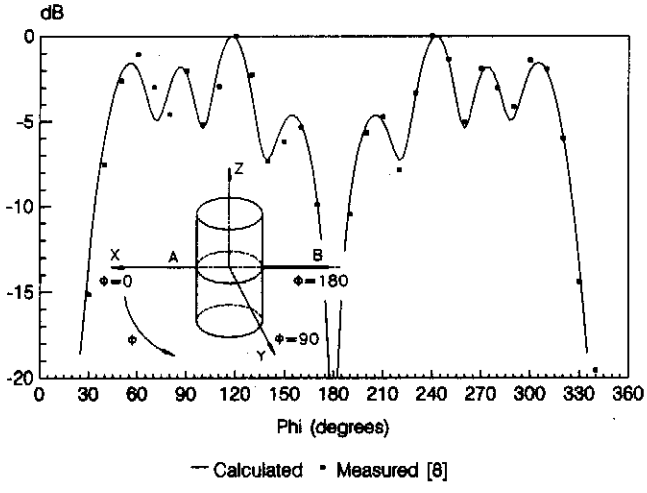

Figure 8. Radiation pattern of a monopole antenna (A) diametrically opposite a passive boom (B)

3.3 Monopole on an polihedrical conducting body

A very special conducting box is shown in Fig.9. A quarterwave monopole antenna is mounted on the top plate of the box (the most narrow). The same figure also includes a sketch of the mesh considered for the box (eight patches per wavelength, the frequency is *317* MHz). The total number of rooftops on the body is *1504*. Figs.10-11 illustrate computed (solid line) and measured (dashed line) values respectively for the $\phi=0^o$ and $\phi=90^o$ cuts, respectively of the radiation patterns. It is important to notice that, although the antenna is very close to the edges of the model the agreement between computed and measured values is relatively good.

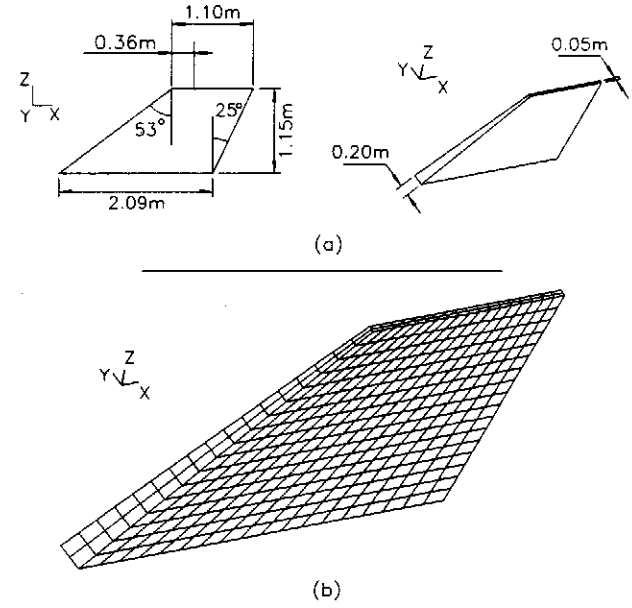

Figure 9. (a) Conducting box with flat sides; (b) Mesh of BP used to model the box

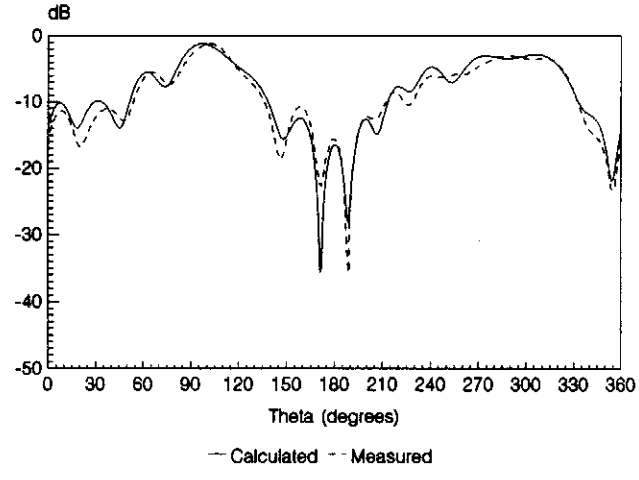

Figure 10. Radiation pattern of a monopole antenna on the top side of the box of Fig. 9 (cut $\phi=0^o$)

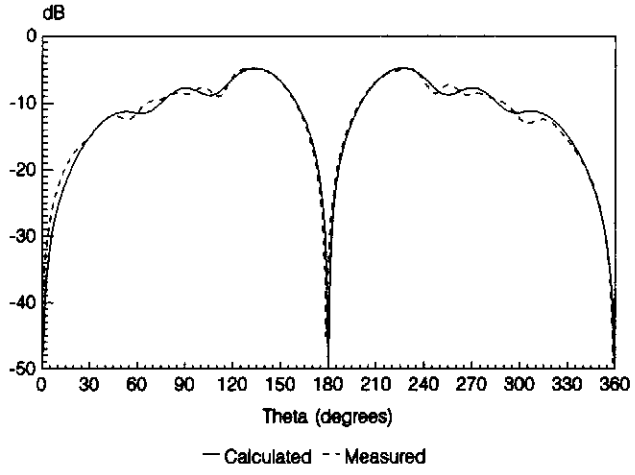

Figure 11. Radiation pattern of a monopole antenna on the top side of the box of Fig. 9 (cut $\phi=90^{o}$)

3.4 Input impedance of a monopole on a box

Fig.12 shows a monopole antenna centred on the top plate of a conducting box. The computed results for the input impedance of this antenna are compared with measurements taken from [11]. Several densities for the mesh of the conducting box have been considered depending on the range of frequencies considered (a number of ten patches per wavelength is always guaranteed). A sketch of the mesh for the frequency band *1.75* to *4.0* GHz is included in the figure. The monopole has been modelled considering *20* subdomains for all the frequency band. A good agreement between calculated and measured data is also observed.

3.5 Input admittance of a monopole on a plane with attached reflected plate

Finally, Fig.13 shows a monopole antenna centred on a conducting flat plate with a reflected plate attached to one side of the ground plane. The mesh considered for all the frequency band is included in the same figure. As in the previous case the monopole has been modelled also by *20* subdomains. The radius of the monopole is *0.0008m*. The computed results for the input admittance of this antenna are compared with measurements taken from [7]. The density for the mesh of the conducting plates that has been considered for all the range of frequencies analyzed is shown in the same figure (a number of ten patches per wavelength is always guaranteed). Good agreement between computed and measured data is observed.

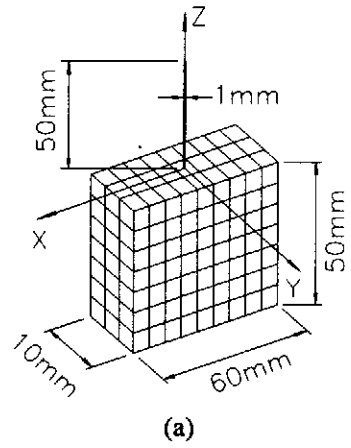

(a)

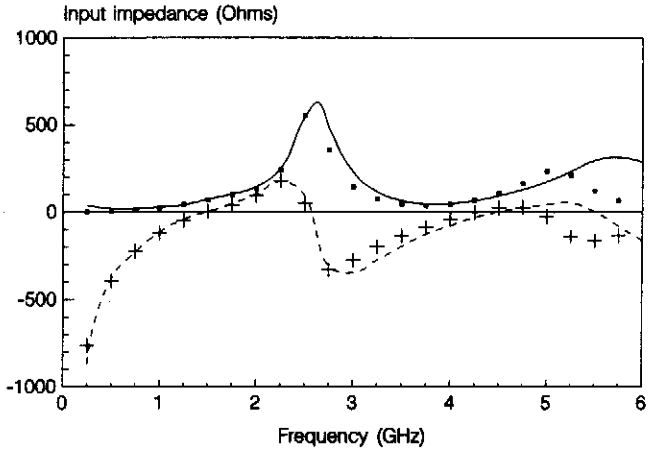

(b)

Figure 12. Monopole antenna on a conducting parallelepiped; (a) meshing of BP for the frequency band *1.75* to *4.0* GHz; (b) results for the input impedance

4 CONCLUSIONS

A new technique based on the MM to analyze antennas on board conducting surfaces has been presented. The scheme makes use of modern computational geometry tools to model the scatterers and the simplicity of wires to model the on-board antennas. This theory has been implemented in a computer code in order to obtain radiation patterns or input impedances of several canonical structures. The wire can be attached to any patch of the body meshing without requiring any special attention. Comparisons between numerical data and measurements show that the method is accurate and efficient for radiation patterns analyses. For input impedance the approach gives reasonably accurate results.

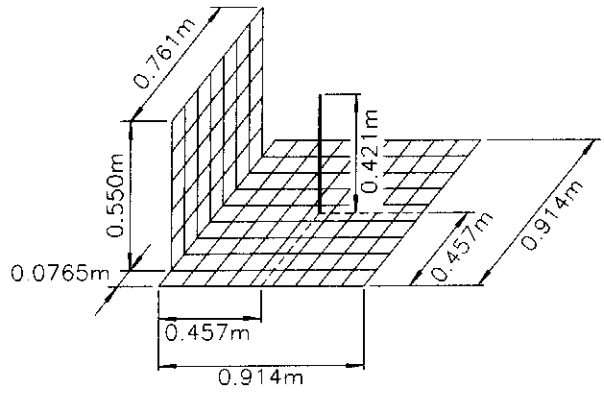

(a)

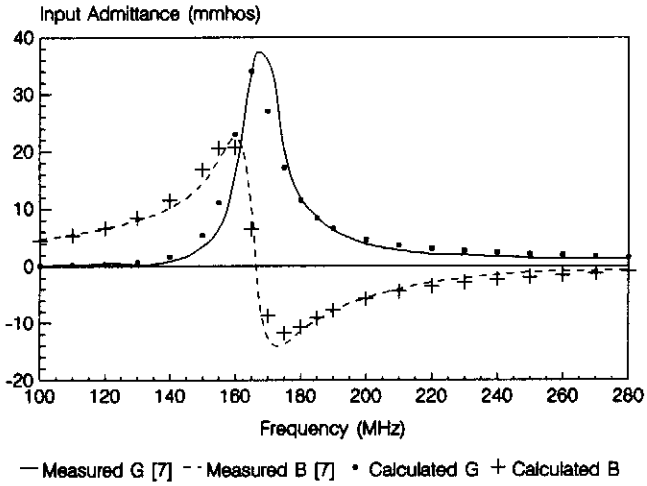

(b)

Figure 13. Monopole antenna on a flat ground plane with attached reflected plate; (a) meshing of BP for all the frequency range; (b) results for the input admittance

ACKNOWLEDGEMENTS

This work was sponsored by CASA and CICYT (Projects No TIC:93-0671- CO6-01, ESP91-0248). Measurements of Figs.10-11 were carried out by INTA.

REFERENCES

[1] R.F. Harrington, "Field Computation by Moment Methods", New York, McMillan, 1968.

[2] J.H. Richmond, "A Wire Grid Model for Scattering by Conducting Bodies", IEEE Transactions on Antennas and Propagation, Vol. AP-14, No. 6, pp. 782-786, November 1966.

[3] G. Farin, "Curves and Surfaces for Computer Aided Geometric Design", Academic Press, INC, 1988.

[4] C. de Boor, "A Practical Guide to Splines", Springer, 1978.

[5] L. Valle, F. Rivas and M.F. Cátedra, "Combining the Moment Method with Geometrical Modelling by NURBS Surfaces and Bézier Patches", IEEE Transactions on Antennas and Propagation, Vol. 42, No. 3, pp. 373-381, March 1994.

[6] A.W. Glisson and D.R. Wilton, "Simple and Efficient Numerical Methods for Problems of Electromagnetic Radiation and Scattering from Surfaces", IEEE Transactions on Antennas and Propagation, Vol. AP-28, No. 5, pp. 593-603, September 1980.

[7] E.H. Newman and D.M. Pozar, "Electromagnetic Modelling of Composite Wire and Surface Geometries", IEEE Transactions on Antennas and Propagation, Vol. AP-26, No. 6, pp. 784-789, November 1978.

[8] N.C. Albertsen, J.E. Hansen and N.E. Jensen, "Computation of Radiation from Wire Antennas on Conducting Bodies", IEEE Transactions on Antennas and Propagation, Vol. AP-22, No. 2, pp. 200-206, March 1974.

[9] J.F. Shaeffer and L.N. Medgyesi-Mitschang, "Radiation from Wire Antennas Attached to Bodies of Revolution: the Junction Problem", IEEE Transactions on Antennas and Propagation, Vol. AP-29, No. 3, pp. 479-487, May 1981.

[10] F.M. Tesche and A.R. Neureuther, "Radiation Patterns for Two Monopoles on a Perfectly Conducting Sphere", IEEE Transactions on Antennas and Propagation, Vol. AP-18, No. 5, pp. 692-694, September 1970.

[11] R. Luebbers, L. Chen, T. Uno and S. Adachi, "Calculation of Radiation Patterns, Impedance and Gain for a Monopole Antenna on a Conducting Box", IEEE Transactions on Antennas and Propagation, Vol. 40, No. 12, pp. 1577-1583, December 1992.